PCCP

Accepted Manuscript

ROYAL SOCIETY OF CHEMISTRY

www.rsc.org/pccp

Thermal spin filter, thermal spin switcher and negative-differential-resistance in thermal spin currents in zigzag SiC Nanoribbons

Dan-Dan Wu[1], Hua-Hua Fu[1, a)], Lei Gu[1], Yun Ni[1], Feng-Xia Zu[1], and Kai-Lun Yao[1, 2]

[1]*College of Physics and Wuhan national high magnetic field center, Huazhong University of Science and Technology, Wuhan 430074, China*

[2] *China Center of Advanced Science and Technology (CCAST), Beijing 100080, China*

Spin caloritronics with a combination of spintronics and thermoelectrics has potential applications in future information science and opens a new direction in the development of multi-functional materials. Based on density functional theory and nonequilibrium Green's function method, we calculate thermal spin-dependent transport through a zigzag silicon carbide nanoribbon (ZSiCNR), which is a heterojunction consisting of left electrode terminated (ZSiC-2H1H) and right electrode terminated (ZSiC-1H1H) by hydrogen. Our results show that when the temperature in the left contact increases over a critical value, the thermal spin-down current increases remarkably from zero, while the thermal spin-up current keeps zero in the total-temperature region, indicating that a perfect thermal spin filter together with a perfect spin switcher is obtained. Furthermore, the thermal spin current shows a negative differential resistance effect and quantum oscillation behaviors. These results suggest that the zigzag SiC nanoribbon proposed by us can be designed as a highly-efficient spin caloritronics device with multiple functionalities.

[a)]Author to whom correspondence should be addressed. Electronic mail: hhfu@mail.hust.edu.cn. Tel./FAX: +86-27-87558512

I. INTRODUCTION

Spin caloritronics, i.e., a combination of spintronics and thermoelectrics, is a research direction that provides alternative strategies for thermoelectric waste heat recovery and cooling.[1,2] A good spin caloritronics material relying on the interplay of heat and charge transport has long attracted attention theoretically and experimentally due to its potential applications in future technologies in green energy and information science.[3-6] The silicon carbide (SiC) has long been considered as an attractive material for numerous technological applications, due to its outstanding properties including high thermal conductivity, high breakdown electric field, high electronic conductivity, excellent chemical and physical stability, good radiation, and wide band gap,[7-8] making it a suitable semiconductor for high-power, high-temperature, high-pressure, and high-frequency devices.[9,10] Furthermore, various lower dimensional SiC structures, such as zero-dimensional nanoparticles and nanosheres, and one-dimensional SiC nanotubes and nanowires, have been already been synthesized experimentally.[11-13] Recently, the theoretical prediction of the stability of two-dimensional (2D) with honeycomb structure have stimulated increasing interest in SiC nanosheets and naribbons (NRs).[14-15] In contrast to graphene,[16] which is essentially a zerogap semiconductor, the 2D monolayer SiC nanosheets and armchair SiC NRs behave as a nonmagnetic wide-band-gap semiconductor due to the ionicity of SiC and the strong spin-orbit coupling,[17-19] whereas zigzag SiCNRs (Z-SiCNRs) are magnetic and can present metallic or semiconducting character,[20,21] depending on the width of the nanoribbon and the types of edge hydrogenation.[22] Besides, *ab inito* investigations have recently shown that these characteristics can be modified or adjusted by the presence of some impurities and defects.[15,22,23] These excellent properties make the SiCNRs promising

candidates for various spintronic device applications.[16,23]

It is natural to ask whether the Z-SiCNRs can be applied as a high-efficient spin caloritronic device and display as good thermoelectric behaviors. Motivated by these, in this work, by means of *ab initio* calculations combined with nonequilibrium Green's function approach, we investigate the thermal spin-dependent transport through a zigzag SiC nanoribbon *N*-ZSiCNR, where the prefix '*N*' represents the number of zigzag chains across the ribbon width. The device model can be considered as a heterojunction consisting of left electrode terminated (*N*-ZSiCNR-2H1H) and right electrode terminated (*N*-ZSiCNR-1H1H) by hydrogen, as illustrated in Figure 1. For convenience, we take $N = 4$ as an example. Our theoretical results show that when the temperature in the left contact increases over a critical value, the thermal spin-down current increases remarkably from zero, while the thermal spin-up current still keeps zero in the total-temperature region, indicating a perfect thermal spin filter together with a perfect spin switcher induced by temperature difference instead of external electrical bias. Furthermore, the thermal spin current performs an obvious negative differential resistance (NDR) effect and quantum oscillation behaviors, indicating that the zigzag SiC nanoribbon proposed by us can be designed as a highly-efficient spin caloritronics device with multiple functionalities, which will put the SiC NRs further toward the device applications in future thermoelectrics possible and provide a new prospect for spin caloritronics and spintronics.

The remainder of this paper is organized as follows. In section 2, we briefly describe model details and computational method. In Section 3, we present the thermoelectric properties, including the thermal spin-filtering effect, the thermal spin-switching effect, and the NDR effect in the thermal spin current flowing through the nanoribbon heterojunction, then discuss

their physical mechanism and further explore their device applications. We conclude the paper in Section 4.

II. DEVICE MODEL AND COMPUTATIONAL METHOD

In the device design, a supercell model is built to study *Z*-SiCNRs with the interlayer distance separated by 30Å to eliminate possible mirror interaction, and the two side edges of the pristine Z-SiCNRs are either terminated by H at Si or C atoms. When the pristine Z-SiCNRs are exposed to H_2 gas, its edge hydrogenation will take place, thus the dangling bonds of Si or C atoms can be eliminated. The edge Si and C atoms are allowed to terminate with either one (sp^2 hybridization) or two (sp^3 hybridization) hydrogen atoms. From *ab initio* calculations,[22] it is found that the different type of hydrogenation and different nanoribbon width perform different magnetic properties. For example, the H-passivated zigzag SiC NRs (Z-SiC-1H1H) narrower than 0.6 nm have only a nonmagnetic semiconducting state, while larger than this critical width are magnetic.[17] Nevertheless, the H-passivated amchair SiC NRs (ASiC-1H1H NRs) are nonmagnetic semiconductors.[24] Furthermore, it is shown that as each edge Si atom is passivated with two H atoms and each edge C atom is passivated with one H atom (Z-SiC-2H1H), the system is magnetic.[17] Considering that Z-SiC-1H1H and Z-SiC-2H1H are two stable structures while possess different magnetic properties, in this work we adopt these two typical structures to construct a heterojunction, in which four dimmer chains across the ribbon width is adopted, as illustrated in Figure 1, which consists of a finite Z-SiCNRs connected to two semi-infinite SiC electrodes, i.e., the left part is 4-Z-SiC-2H1H and the right is 4-Z-SiC-1H1H.

The thermal-spin-current calculations were performed within the framework of the

ATOMISTIX TOOLKIT (ATK) Package,[25,26] which adopts spin density functional theory combined with nonequilibruim Green's function method.[27-29] The core electrons are described by norm-conserving pserdopotentials, and the local-density approximation (LDA) is used for the exchange-correlation potential. Generalized gradient approximation (GGA) exchange-correlation functional delivered similar results, while the convergence of LDA is faster and less computation time is demanded.[30] A single-zeta-polarized (SZP) basis set is used and the cut off energy is 150Ry and a Monkhorst-Pack *k*-mesh of 1×1×100 is chosen in our work. In the Landauer-Büttiker formalism, the spin-dependent current through the system is given by[31,32]

$$I^{\uparrow(\downarrow)} = \frac{e}{h}\int_{-\infty}^{\infty}\left\{T^{\uparrow(\downarrow)}(E)[f_L(E,T_L) - f_R(E,T_R)]\right\}dE, \quad (1)$$

where e is the electron charge, h is the plank constant, $f_{L(R)}(E,T)$ is the equilibrium Fermi-Dirac distribution for the left (right) electrode, $T_{L(R)}$ is the temperature of the left (right) contract, and $T^{\uparrow(\downarrow)}(E)$ is the spin resolved transmittance function and can be defined as

$$T^{\uparrow(\downarrow)}(E) = Tr[\Gamma_L G^R \Gamma_R G^A]^{\uparrow(\downarrow)}, \quad (2)$$

where $G^{R(A)}$ is the retarded (advanced) Green's functions of the central region and $\Gamma_{L(R)}$ is the coupling matrix of the left (right) contact. These expressions will help us obtain the thermal spin-dependent transports through the heterojunction.

In the numerical calculations, geometry optimization and electronic structure calculations are performed with the double numerical plus polarization (DNP) basis set implemented in the DMOL package and ATK.[25,26] The positions of the atoms are relaxed until the maximum force on each atom is no more than 0.01eV/Å. The fist Brilibrium zone is sampled with a 1×4×2, 1×1×100 Monkhorst-pack *k*-point mesh for optimization of SiC supercell and transport

properties calculation, respectively. Two adjacent inplane (out-of-plane) 4-Z-SiCNRs are separated by no more than 10Å to eliminate possible mirror interactions. In addition, the optimization result shows that Si-C distance is 1.781Å, larger than C-C length.

III. RESULTS AND DISUSSION

We calculated the electronic band structures and the density of states (DOS) for different initial settings of spin configurations: non-magnetic, ferromagnetic, and antiferromagnetic, our numerical results show that finally the non-magnetic state is always obtained of the supercell 4-Z-SiC-1H1H and ferromagnetic coupling with the spin polarized edge states of supercell 4-Z-SiC-2H1H. These results are consistent with the consequences that Lou announced in their article.[22]. Therefore, the magnetic state of the heterojunction can be controlled by an external magnetic field. The thermally induced currents are caused by a temperature difference (ΔT) between the temperature of left electrode (T_L) and right electrode (T_R), that is, $\Delta T = T_L - T_R$, without external bias voltage. Simultaneously, we choose the back gate voltage to be fixed at zero, so the carrier concentration and the spin currents are only determined by temperature.

Figure 2(a) shows the calculated thermally induced currents versus T_L of the (4-SiC-2H1H)/(4-SiC-1H1H) heterojunction at different ΔT. One can find that in the low-temperature region of $T_L < 300K$, the heterojunction exhibits a good insulating behavior without any charge or spin current. As the electrode temperature T_L increases over this critical value, the spin-up currents I_{up} nearly keeps zero in the total-temperature region, while the spin-down currents I_{dn} increase remarkably and rises almost linearly, indicating that the spin-down transporting channels are open with increasing of the contact temperature, while the spin-up transporting channels are always forbidden. Obviously, this is a perfect spin filtering

effect together with a spin switching effect, which is generated only from a temperature gradient but not an external bias voltage.[34-36] Nevertheless, in the high-temperature region with T_L > 420K, the situations are much different. For a case of the low temperature difference, taking ΔT = 20K as an example, the thermal spin-down current I_{dn} increases to a limiting one and the curve of I_{dn} - T_L nearly displays as a plateau-like structure, indicating its rectifying behavior in thermal charge current. As ΔT increases to 40K, the curve of I_{dn} - T_L in the high-temperature region shows oscillation behaviors, while as ΔT increases further to a large value, i.e., ΔT=60K, the curve of I_{dn}- T_L shows an obvious NDR effect. To further explore the NDR effect appearing here, we supplement three cases with different temperatures, e.g., ΔT = 55K, 60K and 65K in the region of 410 K< T_L <440 K, and plot them in the inset of Figure 2(a). It is found that the I_{dn} - T_L curve for the case of ΔT = 55K shows obvious oscillating behaviors with a multiple-peak-valley structure, which is caused by a series of small and sharp peaks near the Fermi surface. As ΔT increases to 60K, the oscillating behaviors are much suppressed and only a valley remains around T_L = 430K, and as ΔT increases further, it is interesting that the valley structure is also suppressed and thus the NDR effect disappears in the corresponding temperature. It should be noted that the perfect thermal spin filtering effect, spin switching effect, spin current rectifying effect and the large NDR along with the oscillation behaviors, which were not reported in the similar *N*-Z-SiCNRs device in previous experimental and theoretical works,[37-39] appear simultaneously in the same heterojunction proposed by us, indicating its potential applications in the future spin caloritronics devices. In Figure 2(b), it is shown that the spin-up and spin-down currents with increasing ΔT for T_L = 350, 430 and 500K. Predictably, the spin-down currents I_{dn} increases from zero with the increasing of ΔT and T_L,

while the spin-up currents I_{up} nearly keeps zero for any temperature difference. It is noted that as the left contact is set as T_L = 350K, which is near to the temperature where the NDR effect appears as shown in Figure 2(a), the I_{dn} - ΔT curve presents the nonlinear growth with obvious oscillating behaviors, indicating in these temperatures discrete energy levels exist, which is just the reason why the NDR effect appears in the spin-down current.

From the above discussions, one can find that another advantage of such a Z-SiCNRs heterojunction is the high spin polarizations (SPs) of the thermal spin current. To show this, we plot the spin polarization versus the contact temperature T_L and the temperature difference ΔT, calculated by $SP(\%) = (|I_{up}|-|I_{dn}|)/(|I_{up}|+|I_{dn}|)\times 100$, in Figure 3. It is clearly show that in wide ranges of T_L and ΔT, the spin polarization reaches over 99%. Moreover, both high T_L and large ΔT have contributions to enhance the spin polarizations. Besides, we can see the SP performance is in accordance with the spin current shown in Figure 2. In addition, as for the symmetry-inverted situation ($T_R > T_L$), although our device is not a full symmetric system, the transport curves only show a slight deviation, which could be neglected in application.

In order to explain the high spin polarization and to put a further insight into the thermal spin-dependent transports described above, it is necessary to analyze the density of states (DOS), the band structures and the transmission spectra of the Z-SiCNRs heterojunction. Firstly, DOS of the system, as expected, shows that left electrode consisting of 4-Z-SiC-2H1H behaves as a ferromagnetic semiconductor (see Figure 4(a)), while the right electrode consisting of 4-Z-SiC-1H1H behaves as a nonmagnetic one (see Figure 4(b)). Furthermore, the corresponding band structures of the two electrodes are shown in Figures 4(c) and 4(e). It is obvious that the left electrode shows spin splitting near Fermi surface, and the band gap of the

spin-up is larger than 3.0 eV, presenting insulating properties, while that of the spin-down is nearly 0.26 eV, indicating its semiconductor characteristics. However, it is totally degenerate in the right electrode, and the curve near Fermi surface is smoothly with a stronger bonding as the mergence is larger in the corresponding DOS. As for the spin-dependent transmission spectra plotted in Figure 4(d), it can be found that for spin-up transmission, one narrow channel is open in the energy region [-0.3eV, -0.5eV] and another narrow channel appears in a high energy region [2.5eV, 2.7eV], while a wide channel is open in the energy region [-0.75eV, -1.5eV]. Between them, a wide energy gap, where Fermi surface is localized, appears. While for spin-down transmission, two wide channels appear in the regions [-0.1eV, 0.3eV] and [-1.5eV, -0.2eV], and the first region is crossed over by Fermi surface, which dominates the transport characteristics and produces the perfect spin filtering effect together with the spin switching effect. Moreover, the narrow transmission peaks in the high energy regions induce a series of oscillating behaviors in the high temperatures.

Based on the above descriptions about the band structures and the transmission spectra, we can obtain a clearer physical picture of the emergence of NDR effect in the spin-down current. When $T_L > T_R$, the thermal bias drives spin currents from the left for the right. If near the linear response regime, it is natural to have a positive differential resistance in the spin-down current that increasing T_L will increase the thermal bias which in turn enhances the spin-down current. If we further increases T_L with assuming several levels are totally above the chemical potential, the corresponding states will be totally depleted, which will in turn severely suppress the spin emission process. As a consequence, the spin-down current will decrease although the thermal bias increases. When the thermal conductance decreases faster than the increasing of the

thermal bias, the NDR effect emerges in the thermal spin currents.[40] Nevertheless, these transport phenomena are not found in the spin-up transport, because the spin-up transmitting channels are closed as described in Figure 4.

In addition, it is clear that the above rich thermoelectric transporting behaviors, including the thermal spin filtering, the thermal spin switching and the NDR effect in the thermal spin currents, are tightly associated with the spin splitting in the left part 4-Z-SiC-2H1H. To confirm this, we replace the left part of the heterojunction 4-Z-SiC-2H1H by another structure 4-Z-SiC-2H2H, in which each edge Si or C atom is passivated with two H atoms, while the right part of the heterojunction remains. From the DOS calculations as shown in Figure 5(a), 4-Z-SiC-2H2H nanoribbon is nonmagnetic, which is consistent with the previous results.[20] Moreover, the band structures of the 4-Z-SiC-2H2H nanoribbon are also spin degeneracy but show a gap larger than 0.5 eV around the Fermi level (see Figure 5(c)), indicating its semiconductor characteristic. As for the transmission spectra for this heterojunction plotted in Figure 5(d), one can find that the two wide conductance channels are open in the region [-0.8eV, -0.3eV] and [0.1eV, 0.2eV], respectively. Apart from these, no any additional conductance peaks appear and a wide gap exists around the Fermi level, indicating that the NDR behaviors are difficult to be observed in the current heterojunciton. These band structures and the transmission determine that only when the device temperature T_L increases over a critical value, i.e., the switching temperature T_c = 470K shown in Figure 6, the thermoelectric current begins to flow through the heterojunction. However, for our previous heterojunction (4-Z-SiC-2H1H)/(4-Z-SiC-2H1H), the spin splitting in the left lead makes the gap in the corresponding spin-splitting band structures narrower. As a result, the switching temperature in

it is low to T_c =300K (see Figure 2(a)). These results show that the device design by using the ferromagnetic nanoribbon *N*-Z-SiC-2H1H as one of the contacts is a crucial condition to achieve the spin filtering, the spin switching and the NDR effects in the *N*-Z-SiC nanoribbon heterojunction.

IV. CONCLUSION

In summary, we propose a Z-SiCNRs heterojunction which is composed of ferromagnetic 4-Z-SiC(2H1H) and nonmagnetic 4-Z-SiC(1H1H). By using the first-principle calculations combined with nonequilibrium Green's function approach, the spin-dependent currents induced the thermal bias in two contacts have been investigated. The numerical results show that the thermal spin currents display as a perfect spin filtering effect together with a perfect spin switching effect. Moreover, the thermal spin current performs an unusual NDR effect and oscillation behaviors, indicating that the zigzag SiC nanoribbon proposed by us can be designed as a highly-efficient spin caloritronics device with multiple functionalities, which will put the SiCNRs further toward the device applications in future thermoelectrics possible and provide a new prospect for spin caloritronics and spintronics.

ACKNOWLEDGEMENTS

This work was supported by the National Natural Science Foundation of China (Nos. 11274128, 10804034 and 11074081), by the Natural Science Foundation of Hubei Province (No. 2008CDB003).

[1] S. T. B. Goennenwein and G. E. W. Bauer, Nat. Nanotechnology **7**, 145 (2012).

[2] G. E. W. Bauer, Eiji Saitoh, and Bart J. van Wees, Nat. Mater. **11**, 391 (2012).

[3] M. Zeng, Y. Feng, and G. Liang, Nano Lett. **11**, 1369-1373 (2011).

[4] J. Nakabayashi, D. Yamamote, and S. Kurihara, Phys Rev Lett **102**, 066803 (2009).

[5] W. Y. Kim and K. S. Kim, Nat. Nanotechnology **3**, 408-412 (2008).

[6] M. Zeng, Y. Feng, and G. Liang, Appl. Phys. Lett. **99**, 123114 (2011).

[7] P. Melinon, B. Masenelli, F. Tournus, and A. Perez, Nat. Mater. **6**, 479 (2007).

[8] P. Masri, Surf. Sci. Rep. **48**, 1 (2002).

[9] W. J. Choyke, H. Matsunami, and G. Pensl, *Silicon Carbide: Recent Major advances*, Spring, Berlin, Heidelberg, New York, 2004.

[10] J. M. Morbec and G. Rahman, Phys. Rev. B **87**, 115428 (2013).

[11] P. Lu, Q. Huang, A. Mukherjee, and Y.-L. Hsieh, J. Mater. Chem., **21**, 1005-1012 (2011).

[12] H.-L. Zhu, Y.-J. Bai, R. Liu, N. Lun, Y.-X. Qi, F.-D. Han, and J.-Q. Bi, J. Mater. Chem., 21, 13581-13587 (2011).

[13] X. H. Sun, C. P. Li, W. K. Wong, N. B. Wong, C. S. Lee, S. T. Lee and B. T. Teo, J. Am. Chem. Soc., **124**, 14464-14471 (2002).

[14] H. Sahin, S. Cahangirov, M. Topsakal, E. Bekaroglu, E. Akturk, R. T. Senger, and S. Ciraci, Phys. Rev. B **80**, 155453 (2009)..

[15] E. Bekaroglu, M. Topsakal, S. Cahangirov, and S. Ciraci, Phys. Rev. B **81**, 075433 (2010).

[16] A. H. CastroNeto, F. Guinea, N. M. R. Peres, K. S. Novoselov and A. K. Geim, Rev. Mod. Phys., **81**, 109-162 (2009).

[17] L. Sun, Y. Li, Z. Li, Q. Li, Z. Zhou, Z. Chen, J. Yang and J. G. Hou, J. Chem. Phys., **129**, 174114 (2008).

[18] T.-Y. Lü, X.-X. Liao, H.-Q. Wang and J.-C. Zheng, J. Mater. Chem., 22, 10062-10068 (2012).

[19] X. Liu, S. Lin, Y. Xu, A. A. Hakro, T. Hasan, B. Zhang, B. Yu, E. Li, J. Luo, and H. Chen, J. Mater. Chem. C, **1**, 2131-2135 (2013).

[20] P. Lou and J. Y. Lee, J. Phys. Chem. C **113**, 12637 (2009).

[21] J.-M. Zhang, F.-L. Zheng, Y. Zhang, and V. Ji, J. Mater. Sci. **45**, 3259 (2010).

[22] P. Lou, J. Mater. Chem. C **1**, 2996 (2013).

[23] C. D. Costa and J. M. Morbec, J. Phys.: Condens. Matter **23**, 205504 (2011).

[24] E. Bekaroglu, M. Topsakal, S. Cahangirov, and S. Ciraci, Phys. Rev. B **81**, 075433 (2010).

[25] Atomistix ToolKit, 2008.02, see http://quantumwise.com/.

[26] J. Taylor, H. Guo, and J. Wang, Phys. Rev. B **63**, 245407 (2001).

[27] H. H. Fu and K. L. Yao, Appl. Phys. Lett. **100**, 013502 (2012).

[28] H. H. Fu and K. L. Yao, J. Chem. Phys.**134**, 054903 (2011).

[29] H. H. Fu and K. L. Yao, J. Appl. Phys. **110**, 094502 (2011).

[30] O. V. Yazyev and L. Helm, Phys. Rev. B **75**, 125408 (2007).

[31] M. Büttiker, Y. Imry, R. Landauer, and S. Pinhas, Phys. Rev. B **31**, 6207 (1985).

[32] M. Brandbyge, J. L. Mozos, P. Ordejon, J. Taylor, and K. Stokbro, Phys. Rev. B **65**, 165401-165417 (2002).

[33] H. Li, L. Wang, Q. Liu, and J. Zheng, Eur. Phys. J. B **85**, 274 (2012).

[34] G. Papp and F. M. Peeters, Appl. Phys. Lett., **78**, 2184 (2001).

[35] P. Středa and P. Šeba. Phys. Rev. Lett. **90**, 256601 (2003).

[36] J. C. Egues, C. Gould, G. Richter, and L. W. Molenkam, Phys. Rev. B **64**, 195319 (2001).

[37] F. Giazotto, T. T. Heikkilä, A. Luukanen, A. M. Savin and J. P. Pekola, Rev. Mod. Phys., **78**, 217-274 (2006).

[38] Y. Dubi and M. Di Ventra, Rev. Mod. Phys., **83**, 131-155 (2011).

[39] M. Wierzbowska and A. Dominiak, arXiv: 1403-4989v1 [cond-mat.mtrl-sci] 19 Mar 2014.

[40] J. Ren and J.-X. Zhu, Phys. Rev. B **87**, 241412(R) (2013).

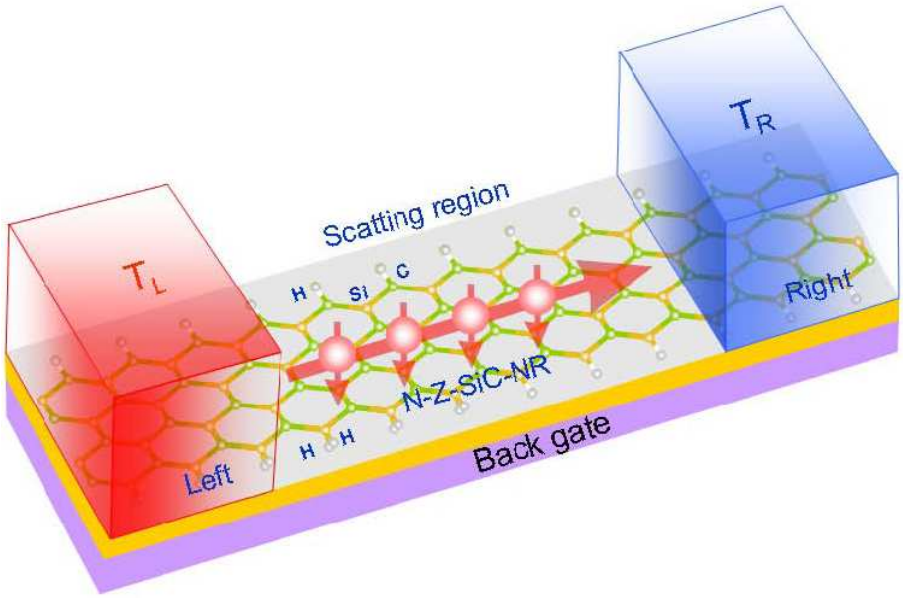

FIG. 1. The schematic illustration of the thermal spin caloritronics device based on (4-Z-SiC-2H1H)/ (4-Z-SiC-1H1H) heterojunction. The spin-dependent currents are induced by ΔT, the temperature difference between the left electrode (T_L) and the right electrode (T_R), that is, $\Delta T = T_L - T_R$.

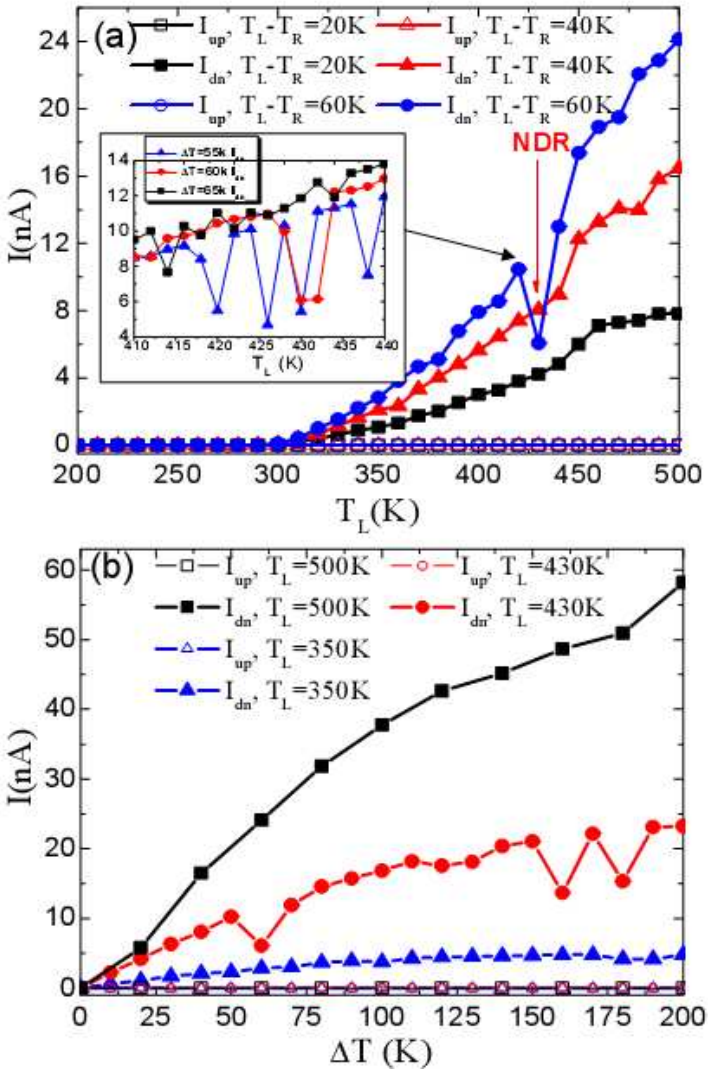

FIG. 2. The thermal spin-dependent currents versus T_L are shown in Figure (a), where the temperature difference ΔT is set as 20K, 40K and 60K, and the set in it shows the spin-down current with ΔT = 55K, 60K and 65K in the region of 410K < T_L < 440K. The thermal spin-dependent currents versus ΔT are shown in Figure (b), where the temperature in the left contact is T_L = 350K, 430K and 500K.

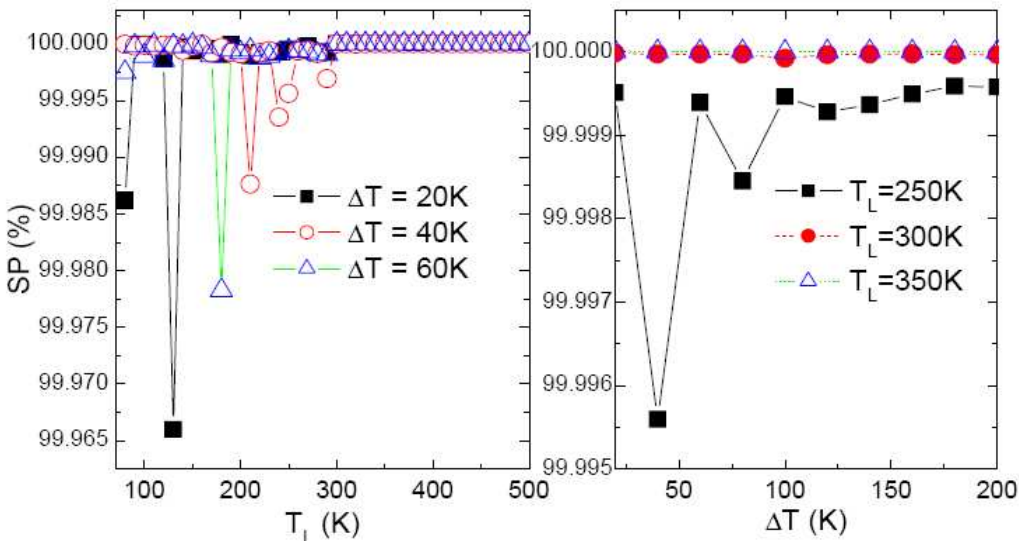

FIG. 3. The spin polarizations as a function of T_L (a) and as a function of ΔT (b), calculated by the relation SP (%)=($|I_{up}|$-$|I_{dn}|$)/($|I_{up}|$+$|I_{dn}|$)×100.

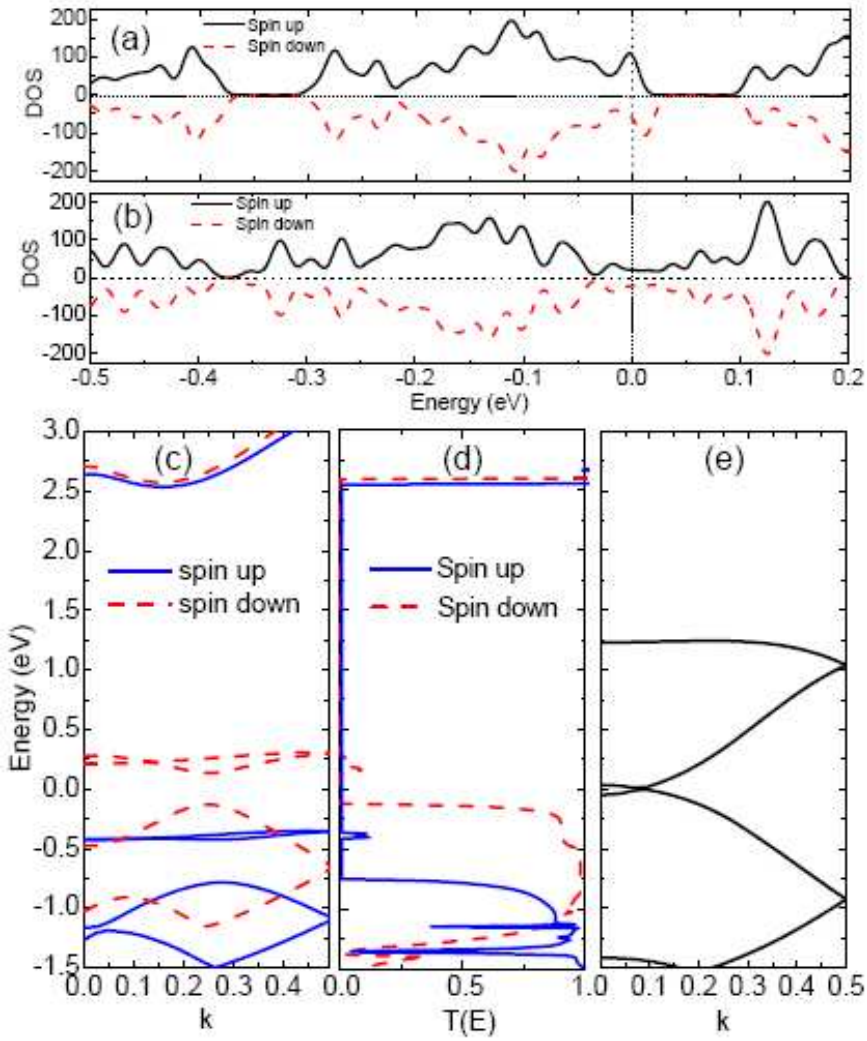

FIG. 4. DOS of the 4- Z-SiC-2H1H region and the 4-Z-SiC-1H1H region are shown in Figure (a) and (b), respectively. Band structures of the left electrode 4-Z-SiC-2H1H and the right electrode 4-Z-SiC-1H1H are shown in Figure (c) (left panel) and (e) (right panel), the corresponding transmission spectra are drawn in Figure (d) (middle panel).

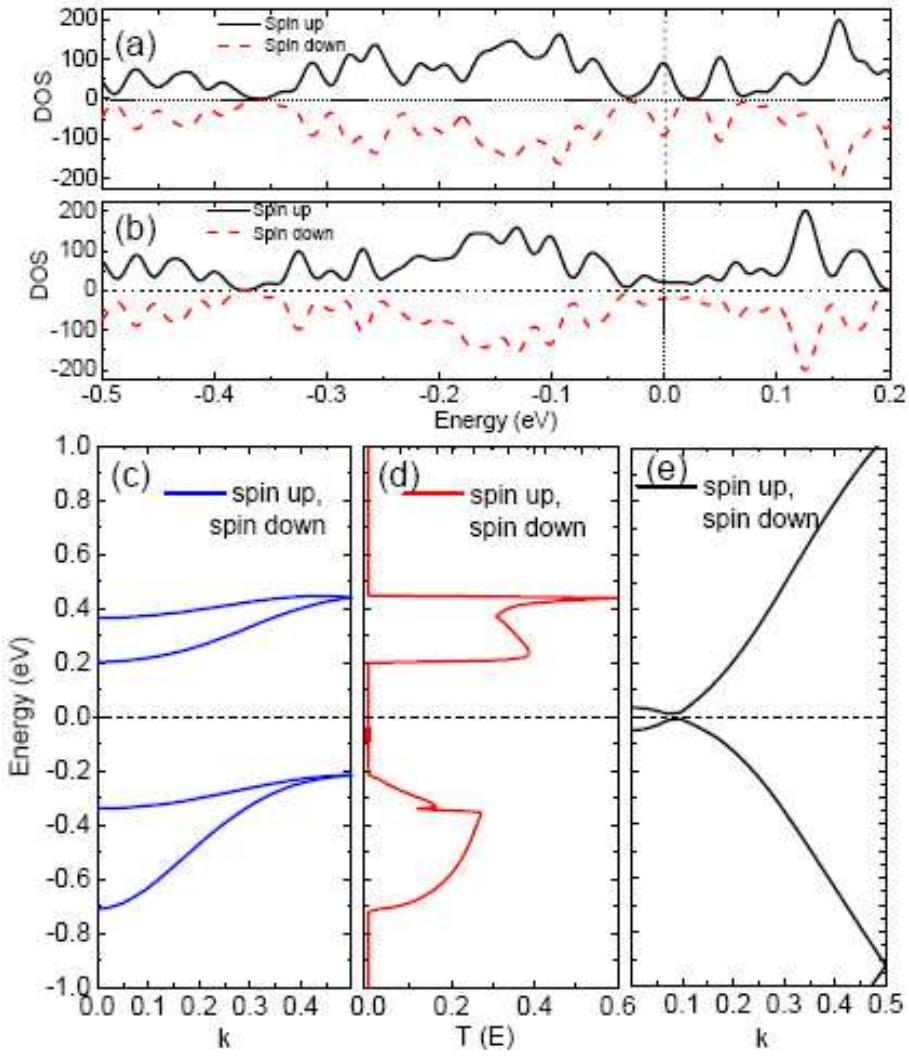

FIG. 5. DOS of the 4- Z-SiC-2H2H region and the 4-Z-SiC-1H1H region are shown in Figure (a) and (b), respectively. Band structures of the left electrode 4-Z-SiC-2H2H and the right electrode 4-Z-SiC-1H1H are shown in Figure (c) (left panel) and (e) (right panel), the corresponding transmission spectra are drawn in Figure (d) (middle panel).

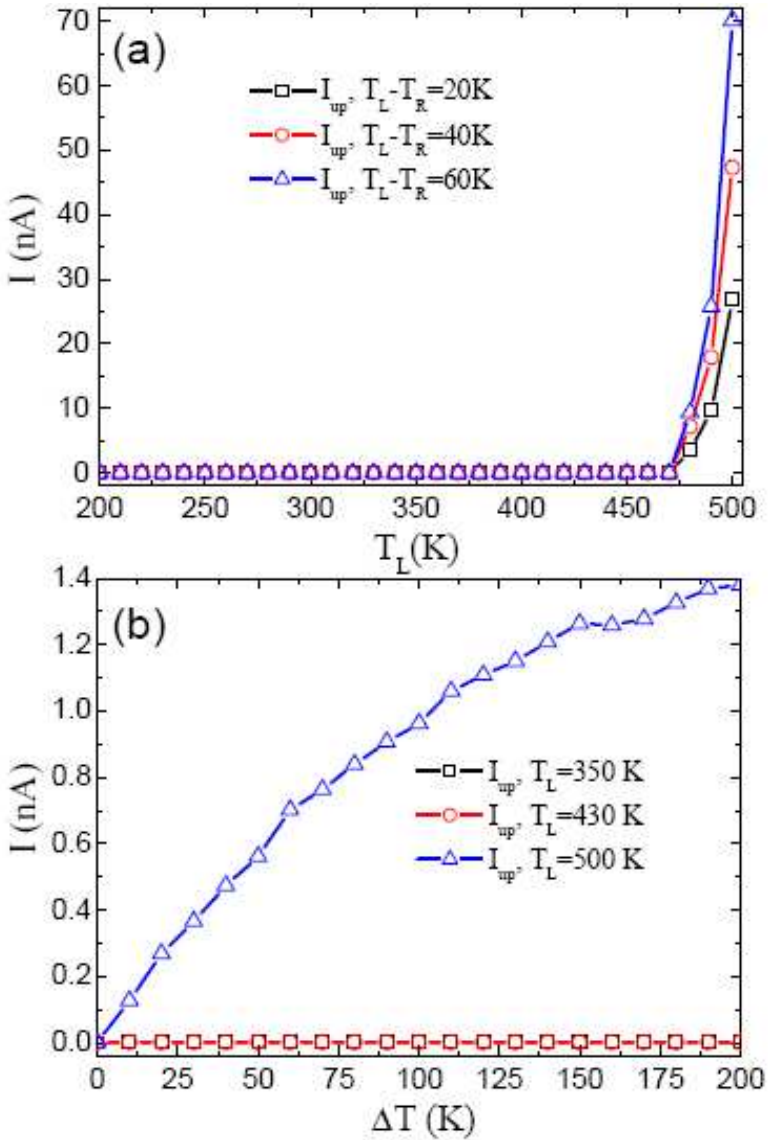

FIG. 6. The thermal spin-up currents through the heterojunction (4-Z-SiC-2H2H) /(4-Z-SiC-1H1H) versus T_L are shown in Figure (a), where the temperature difference ΔT is set as 20K, 40K and 60K. The thermal spin-up currents versus ΔT are shown in Figure (b), where the temperature in the left contact is T_L = 350K, 430K and 500K. Due to the left and right leads are nonmagnetic, the currents are spin degenerate and only the spin-up currents are plotted.

A table of contents entry

(1) Colour graphic:

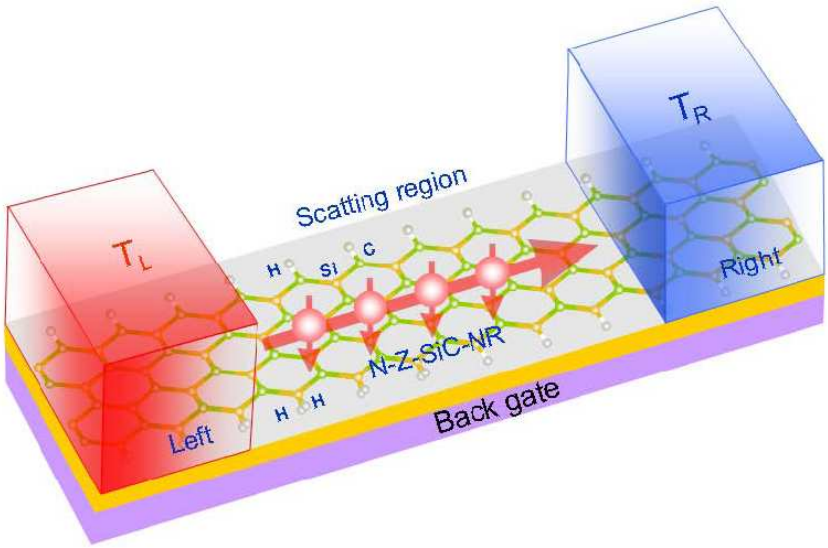

(2) Highlighting:

A thermoelectric heterojunction device based on zigzag silicon carbide narnribbons can be served as perfect thermal spin filter and switcher.